Uncertainty-Aware Adaptive Control for Human-Centric Cyber-Physical Indoor Spaces*

Zahra Elmi[1], Soheila Elmi[2], and Semira Elmi[3]

***Abstract*— This paper presents an uncertainty-aware adaptive control framework for indoor HVAC operation under occupancy uncertainty. The method combines a quantile-regression occupancy predictor with conformal calibration, a PMV-based Random Forest thermal-comfort classifier, and a risk-averse interval MPC operating on an identified RC thermal/IAQ model. The occupancy module achieves an MAE of 0.0326 persons with empirical 95% prediction-interval coverage of 0.9516 and mean interval width of 0.3463 persons. The comfort classifier achieves 0.8387 accuracy, 0.8557 balanced accuracy, and 0.8345 Macro-F1. In a 7-day closed-loop evaluation using real operational building data, the proposed UA-MPC reduces temperature violations from 47 to 30 and CO2 violations from 47 to 29 relative to a certainty-equivalent MPC, at a 23.5% energy overhead versus CE-MPC but with 92.7% lower energy use than a rule-based controller. Additional analysis over five representative two-day windows suggests that these gains are not limited to a single operating window. These results position UA-MPC as a robust comfort- and IAQ-oriented alternative to deterministic building control under uncertain occupancy.**

I. Introduction

Buildings are increasingly operated as cyber-physical systems in which sensing, forecasting, and supervisory control interact in a closed loop. Occupancy is a major exogenous driver in this setting because it affects internal heat gains, ventilation demand, indoor CO_2 generation, and the relevance of comfort-oriented control actions. However, zone-level occupancy is rarely available at the temporal and spatial resolution required by advanced controllers and is often inferred from indirect signals such as passive infrared sensing, CO_2, light, sound, environmental measurements, or multimodal sensor combinations [1], [2], [4].

Recent occupancy-sensing studies have produced richer datasets and more accurate machine-learning predictors [2], [3], [1]. Nevertheless, many building-control pipelines still reduce occupancy to a deterministic schedule or a single point forecast. This simplification can lead to unnecessary energy use when occupancy is overestimated and to avoidable comfort or indoor-air-quality (IAQ) violations when occupancy is underestimated [7], [8], [9], [10]. Model predictive control (MPC) is well suited to smart-building operation because it explicitly handles multivariable dynamics, constraints, and energy–comfort trade-offs [6], [8], [9], [10]. In parallel, occupant-centric control emphasizes that supervisory decisions should reflect actual human presence rather than static schedules [7]. Data-driven thermal-comfort models based on resources such as ASHRAE Global Thermal Comfort Database II further support human-centered control, while conformal prediction provides a practical mechanism for obtaining empirically calibrated uncertainty intervals [12], [13], [5]. However, calibrated occupancy uncertainty is still rarely propagated directly into MPC together with comfort and IAQ objectives [11].

This paper proposes an uncertainty-aware adaptive control framework for human-centric cyber-physical indoor spaces. The contribution is not the isolated use of quantile regression, conformal prediction, Random Forest classification, or MPC. Rather, the contribution is their control-oriented integration: calibrated occupancy intervals are propagated into a risk-averse interval MPC, PMV-based comfort probabilities modulate temperature-violation penalties, and architect-informed spatial priorities differentiate zones according to operational importance. The resulting UA-MPC framework is evaluated in an offline closed-loop setting against certainty-equivalent and rule-based baselines, quantifying both robustness gains and the associated energy cost.

Notation and Preliminaries

Let $i \in \{1, \dots, M\}$ denote the zone index and t the discrete control time index. The vectors $\mathbf{T}_t = [T_{1,t}, \dots, T_{M,t}]^\top$ and $\mathbf{C}_t = [C_{1,t}, \dots, C_{M,t}]^\top$ collect zone temperatures and CO_2 concentrations, and the system state is $\mathbf{x}_t = [\mathbf{T}_t^\top, \mathbf{C}_t^\top]^\top$. The vector $\mathbf{u}_t$ denotes HVAC and ventilation inputs, $\mathbf{n}_t$ denotes zone-wise occupancy, and $\mathbf{d}_t$ contains known exogenous disturbances. The occupancy predictor provides the median forecast $\hat{\mathbf{n}}_{0.50,t+k|t}$ and calibrated bounds $\underline{\mathbf{n}}^c_{t+k|t}$ and $\overline{\mathbf{n}}^c_{t+k|t}$ over horizon H. The scalar α controls the occupancy risk bias, ϕ_i is the spatial priority of zone i, and $\xi^T_{i,t+k|t}$ and $\xi^C_{i,t+k|t}$ denote temperature and CO_2 slack variables.

II. Related Work

A. Occupancy Sensing, Datasets, and Prediction

Occupancy sensing in buildings has evolved from binary presence detection toward occupant-count estimation using environmental and multimodal signals such as passive infrared sensing, CO_2, temperature, humidity, light, smart-meter data, thermal or RGB cameras, and audio streams [1], [14]. Public datasets, including the Room Occupancy Estimation dataset and the high-fidelity multimodal dataset of Jacoby *et al.*, have supported this shift toward more

*This work was not supported by any organization

[1]Zahra Elmi is with the Department of Software Engineering, Faculty of Engineering, Beykoz University, Istanbul, Turkey zehraelmi@beykoz.edu.tr

[2]Soheila Elmi is with the Department of Electrical and Electronics Engineering, Koç University, Istanbul, Turkey selmi24@ku.edu.tr

[3]Semira Elmi is with the Faculty of Fine Arts, Graphic Design, Beykent University, Istanbul, Turkey 2520078007@student.beykent.edu.tr

realistic occupancy modelling [3], [2]. Environmental sensing remains attractive because it is low-cost and privacy-preserving, but its relation to true occupancy can be affected by ventilation settings, window opening, and other operational factors [4]. Although recent work has improved occupancy estimation by incorporating variables such as ventilation-system state and differential pressure [4], most studies still emphasize point-estimation accuracy or sensor-fusion performance rather than calibrated uncertainty for downstream supervisory control. Conformal prediction offers a practical route toward empirically calibrated intervals, yet calibrated occupancy uncertainty remains weakly integrated into occupancy-aware MPC [5].

B. Occupant-Centric and Uncertainty-Aware Control

MPC is widely used in smart-building operation because it can explicitly handle multivariable dynamics, constraints, and energy–comfort trade-offs [6]. In parallel, occupant-centric control argues that building operation should respond to actual human presence and usage patterns rather than fixed schedules or equipment-level heuristics [7]. Robust and stochastic MPC formulations have addressed uncertainty in weather, disturbances, model mismatch, or humidity dynamics [8], [9], [10], and recent occupant-centric studies have jointly considered comfort, air quality, and energy management using real-time occupant-related information [15], [16], [17]. However, the dominant uncertainty sources in this literature are still typically weather forecasts, generic disturbances, or model uncertainty rather than calibrated occupancy uncertainty itself. This distinction matters because occupancy directly affects internal heat gains, ventilation demand, CO_2 generation, comfort relevance, and the penalty structure of supervisory-control decisions.

C. Thermal Comfort, IAQ, and Human-Centered Objectives

Thermal comfort modelling has shifted from analytical indices toward data-driven inference. ASHRAE Global Thermal Comfort Database II has enabled large-scale modelling of subjective comfort responses from environmental and personal variables [12], [13]. Despite this progress, many supervisory-control studies still represent comfort through static temperature bands, while others treat thermal comfort and IAQ separately rather than within a unified decision-making framework [13], [11]. Recent occupant-centric control studies show the value of jointly considering comfort, IAQ, and energy performance, but they do not fully address how calibrated human-related uncertainty should be propagated into the control problem [15], [16], [11].

D. Positioning of the Present Study

The reviewed literature establishes four foundations: occupancy sensing and prediction, occupant-centric building control, uncertainty-aware MPC, and data-driven comfort modelling [1], [7], [6], [13]. The present paper does not claim novelty in quantile regression, conformal prediction, Random Forest classification, or MPC as isolated methods. Instead,

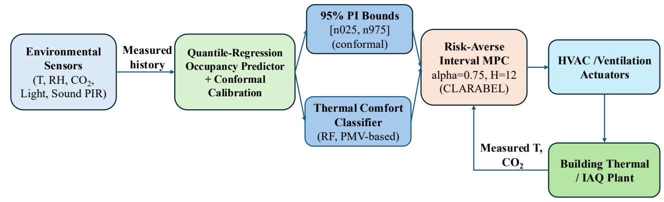

Fig. 1: Overall architecture of the proposed UA-MPC framework. Calibrated occupancy intervals and PMV-based comfort information are propagated to the risk-averse MPC together with state feedback from the identified thermal/IAQ plant.

its contribution lies in their control-oriented integration. Existing occupancy-prediction studies mainly emphasize sensing modality, count-estimation accuracy, or point-forecast performance, whereas this work uses calibrated prediction intervals as control inputs. Existing robust or stochastic MPC studies commonly address weather, generic disturbances, or model uncertainty, whereas this work focuses on calibrated occupancy uncertainty as a driver of thermal and IAQ risk. Existing comfort-aware control studies often use static temperature bands or comfort indicators separately from IAQ constraints, whereas the proposed framework embeds PMV-based comfort probabilities, CO_2 limits, and zone priorities within one supervisory MPC objective. Thus, the contribution is a unified MPC framework that integrates calibrated occupancy uncertainty, comfort-aware penalty modulation, and architect-informed spatial prioritization for human-centric indoor operation.

III. Uncertainty-Aware MPC Framework

Fig. 1 summarizes the proposed uncertainty-aware model predictive control (UA-MPC) framework. The method combines three components: conformalized occupancy prediction, PMV-based thermal-comfort inference, and risk-averse interval MPC on an identified reduced-order thermal/IAQ model. The design preserves calibrated occupancy uncertainty until the control layer, rather than reducing occupancy to a single deterministic forecast.

A. System Model and Risk-Biased Occupancy Input

We consider a building divided into M thermal zones. For zone i, the controller monitors indoor temperature $T_{i,t}$ and CO_2 concentration $C_{i,t}$ at discrete time t, with control interval $\Delta t = 15$ min. Let

$$\mathbf{T}_t = [T_{1,t}, \ldots, T_{M,t}]^\top, \qquad \mathbf{C}_t = [C_{1,t}, \ldots, C_{M,t}]^\top,$$

and define the aggregated state as

$$\mathbf{x}_t = \begin{bmatrix} \mathbf{T}_t^\top & \mathbf{C}_t^\top \end{bmatrix}^\top. \tag{1}$$

The identified reduced-order thermal/IAQ model is

$$\mathbf{x}_{t+1} = \mathbf{A}\mathbf{x}_t + \mathbf{B}\mathbf{u}_t + \mathbf{E}\mathbf{n}_t + \mathbf{F}\mathbf{d}_t + \mathbf{w}_t, \tag{2}$$

where $\mathbf{u}_t$ denotes HVAC and ventilation inputs, $\mathbf{n}_t$ is the zone-wise occupancy vector, $\mathbf{d}_t$ contains known exogenous disturbances, and $\mathbf{w}_t$ captures residual model mismatch. The matrices $\mathbf{A}$, $\mathbf{B}$, $\mathbf{E}$, and $\mathbf{F}$ represent state propagation, control effects, occupancy-driven heat/CO_2 gains, and known disturbance effects, respectively. The controlled output is

$$\mathbf{y}_t = \mathbf{C}\mathbf{x}_t, \tag{3}$$

where $\mathbf{y}_t$ contains the temperature and CO_2 variables used by the supervisory controller.

The occupancy predictor provides the median forecast $\hat{\mathbf{n}}_{0.50,t+k|t}$ and calibrated bounds $\underline{\mathbf{n}}^c_{t+k|t}$ and $\overline{\mathbf{n}}^c_{t+k|t}$ over horizon $H = 12$. Since underestimating occupancy can increase thermal discomfort and CO_2 violations, the MPC uses a risk-biased trajectory

$$\tilde{\mathbf{n}}^{(\alpha)}_{t+k|t} = \hat{\mathbf{n}}_{0.50,t+k|t} + (2\alpha - 1)\left(\overline{\mathbf{n}}^c_{t+k|t} - \hat{\mathbf{n}}_{0.50,t+k|t}\right), \quad \alpha \in [0.5, 1]. \tag{4}$$

Here, $\alpha = 0.5$ corresponds to median occupancy operation, whereas $\alpha = 1.0$ uses the calibrated upper bound. The value $\alpha = 0.75$ is used as an intermediate risk-averse setting between certainty-equivalent and fully conservative operation.

B. Risk-Averse MPC Objective

At each time step, the MPC minimizes the finite-horizon cost

$$J_t = \sum_{k=0}^{H-1} \ell_{t+k|t}, \tag{5}$$

with stage cost

$$\ell_{t+k|t} = \lambda_E P_{t+k|t} + \lambda_T \sum_{i=1}^{M} \phi_i \omega^{\mathrm{PMV}}_{i,t+k|t} \xi^T_{i,t+k|t} + \lambda_C \sum_{i=1}^{M} \phi_i \xi^C_{i,t+k|t} + \lambda_\Delta \left\| \mathbf{u}_{t+k|t} - \mathbf{u}_{t+k-1|t} \right\|_2^2. \tag{6}$$

The four terms penalize energy use, temperature violations, CO_2 violations, and rapid control changes, respectively. The slack variables $\xi^T_{i,t+k|t}$ and $\xi^C_{i,t+k|t}$ soften thermal and IAQ constraints. The spatial priority ϕ_i adjusts the penalty according to zone function, while $\omega^{\mathrm{PMV}}_{i,t+k|t}$ increases the temperature-violation penalty when the predicted comfort state is non-neutral.

The MPC is subject to

$$\mathbf{x}_{t+k+1|t} = \mathbf{A}\mathbf{x}_{t+k|t} + \mathbf{B}\mathbf{u}_{t+k|t} + \mathbf{E}\tilde{\mathbf{n}}^{(\alpha)}_{t+k|t} + \mathbf{F}\mathbf{d}_{t+k|t}, \tag{7}$$

$$\underline{\mathbf{u}} \le \mathbf{u}_{t+k|t} \le \overline{\mathbf{u}}, \tag{8}$$

$$\underline{T}_i - \xi^T_{i,t+k|t} \le T_{i,t+k|t} \le \overline{T}_i + \xi^T_{i,t+k|t}, \quad \forall i, \tag{9}$$

$$C_{i,t+k|t} \le C_i^{\max} + \xi^C_{i,t+k|t}, \quad \forall i, \tag{10}$$

$$\xi^T_{i,t+k|t}, \xi^C_{i,t+k|t} \ge 0, \quad \forall i. \tag{11}$$

These constraints define state propagation, actuator limits, soft temperature limits, soft CO_2 limits, and nonnegative violation magnitudes. The certainty-equivalent MPC baseline uses the same model, horizon, constraints, objective terms, and solver settings, but replaces $\tilde{\mathbf{n}}^{(\alpha)}_{t+k|t}$ with the median forecast $\hat{\mathbf{n}}_{0.50,t+k|t}$.

C. Occupancy Prediction With Conformal Calibration

The occupancy module uses environmental measurements, including temperature, relative humidity, CO_2, light intensity, and related indoor signals, to forecast future occupant count. For each horizon step $t + k$, the quantile-regression model outputs $\hat{n}_{0.025,t+k|t}$, $\hat{n}_{0.50,t+k|t}$, and $\hat{n}_{0.975,t+k|t}$ by minimizing the pinball loss

$$\mathcal{L}_q(y, \hat{y}_q) = \max\left(q(y - \hat{y}_q), (q-1)(y - \hat{y}_q)\right). \tag{12}$$

Raw quantile regression estimates conditional quantiles but does not guarantee empirical interval coverage on finite test data. To obtain calibrated intervals, split conformal calibration is applied on a held-out calibration set. For calibration sample j, the nonconformity score is

$$s_j = \max\left\{\hat{n}_{0.025}(x_j) - y_j,\ y_j - \hat{n}_{0.975}(x_j),\ 0\right\}. \tag{13}$$

The conformal correction is

$$q_\delta = \mathrm{Quantile}_{1-\delta}\left(\{s_j\}_{j=1}^{N_{\mathrm{cal}}}\right), \tag{14}$$

and the calibrated interval is

$$\underline{n}^c_{t+k|t} = \hat{n}_{0.025,t+k|t} - q_\delta, \tag{15}$$

$$\overline{n}^c_{t+k|t} = \hat{n}_{0.975,t+k|t} + q_\delta. \tag{16}$$

These bounds define the interval used to construct the risk-biased trajectory in (4). As shown in Fig. 2, the occupancy module achieves an MAE of 0.0326 persons, empirical 95% coverage of 0.9516, and mean interval width of 0.3463 persons.

D. PMV-Based Comfort and Spatial Priority

The comfort module maps indoor environmental conditions to three PMV-based classes: *Cool*, *Neutral*, and *Warm*. It is trained on ASHRAE Global Thermal Comfort Database II using air temperature, relative humidity, air velocity, clothing insulation, and metabolic rate. A Random Forest classifier is adopted because these inputs are structured tabular variables, and tree ensembles can capture nonlinear feature interactions with limited tuning.

The classifier produces class probabilities $p^{\mathrm{cool}}_{i,t+k|t}$, $p^{\mathrm{neutral}}_{i,t+k|t}$, and $p^{\mathrm{warm}}_{i,t+k|t}$. These probabilities define

$$\omega^{\mathrm{PMV}}_{i,t+k|t} = 1 + \beta\left(p^{\mathrm{cool}}_{i,t+k|t} + p^{\mathrm{warm}}_{i,t+k|t}\right), \tag{17}$$

where $\beta = 1$ in this study. Thus, predicted *Cool* or *Warm* states increase the temperature-slack penalty, whereas predicted *Neutral* states retain the base penalty. Fig. 3 reports an accuracy of 0.8387, balanced accuracy of 0.8557, and macro-F1 score of 0.8345.

Spatial priorities are introduced through ϕ_i in (6). The weights in Table I are function-based design priors rather than learned parameters. Meeting rooms receive higher priority because they typically have higher occupant density,

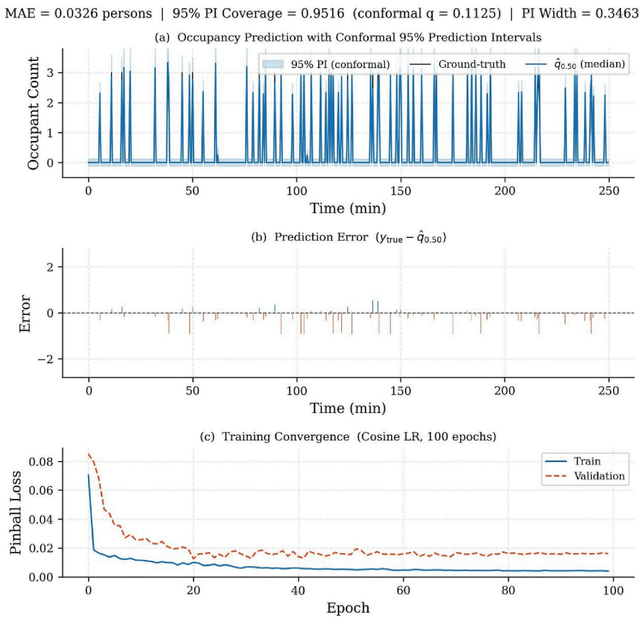

Fig. 2: Quantile-regression occupancy prediction with split conformal calibration.

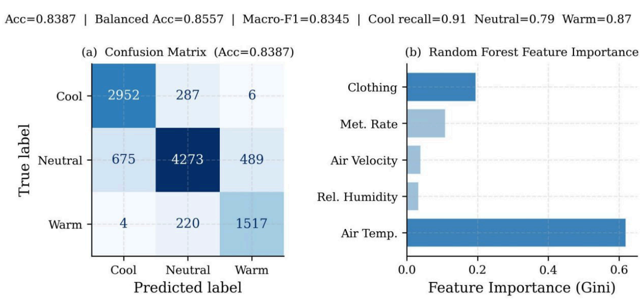

Fig. 3: PMV-based thermal-comfort classification on ASHRAE DB II.

longer seated exposure, and lower tolerance to comfort or IAQ degradation. Corridors receive lower priority because occupancy is usually transient.

A violation in a meeting room therefore contributes more to the MPC objective than the same numerical violation in a corridor. The priority mechanism is transparent and can be adjusted according to local operating policies.

IV. Experimental Setup and Results

A. Data and Evaluation Protocol

The empirical pipeline combines public datasets and operational building data for three complementary tasks. The UCI Occupancy Detection dataset and the Room Occupancy Estimation dataset are used for occupancy-modeling development, ASHRAE DB II is used for thermal-comfort classification, and the supervisory-control layer is evaluated in offline closed-loop simulation using real operational building data with an identified reduced-order RC thermal/IAQ model derived from the LBNL Building 59 setting.

TABLE I: Function-based spatial priority priors.

Zone Type	ϕ	Temp. Band (°C)	CO_2 Limit
Meeting Room	1.5	21.0–24.0	900
Open Office	1.0	20.5–24.5	1000
Corridor	0.5	19.0–26.0	1200

The RC thermal/IAQ model is identified on a training portion of the operational data and validated on temporally separated held-out periods. Validation is performed using one-step prediction error and short free-run simulations for both temperature and CO_2 states. The residual term $\mathbf{w}_t$ in (2) therefore represents the remaining mismatch after model identification, including unmodeled disturbances and sensor noise. To prevent model mismatch from dominating the uncertainty analysis, UA-MPC and CE-MPC are evaluated with the same identified model, horizon, constraints, objective terms, and solver settings. The comparison, therefore, isolates the effect of propagating calibrated occupancy uncertainty rather than confounding it with different plant models or controller structures. The identified model achieved held-out validation errors of 0.24 °C RMSE for temperature and 41.7 ppm RMSE for CO_2. These errors were small relative to the temperature comfort bands and CO_2 limits enforced in the MPC, indicating that the reduced-order model was sufficiently accurate for supervisory prediction. Three controllers are compared throughout the study: **UA-MPC**, the proposed uncertainty-aware controller using conformalized occupancy intervals and architect-informed spatial priorities; **CE-MPC**, a certainty-equivalent controller with the same identified model, objective structure, and horizon but using only the median occupancy forecast; and **Rule-Based**, a fixed-threshold supervisory baseline that reacts to temperature and CO_2 conditions without predictive occupancy information.

Evaluation is reported at three levels. First, representative two-day windows are used to visualize controller behavior under different occupancy regimes. Second, a continuous seven-day aggregate evaluation summarizes the overall comfort–IAQ–energy trade-off. Third, mean ± standard deviation over five two-day windows is reported to assess cross-scenario consistency. The five-window analysis is not intended to replace the continuous seven-day evaluation; rather, it complements it by exposing how controller performance varies across shorter operating periods with different occupancy timing and intensity. The windowed summary preserves temporal interpretability while still sampling multiple operating conditions with different occupancy timing and intensity. Violation counts are reported in occupied 15-min control steps; accordingly, 200 occupied steps correspond to 50 occupied hours.

B. Upstream Model Performance

Before assessing closed-loop control, it is necessary to establish that the two upstream learning modules provide sufficiently reliable inputs to the supervisory pipeline. As shown in Fig. 2, the occupancy predictor combines low point

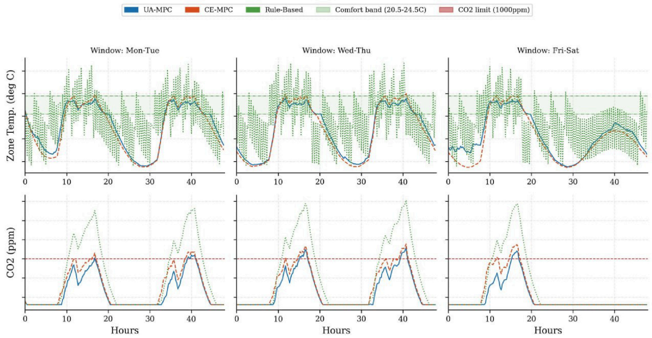

Fig. 4: Representative two-day windows comparing UA-MPC, CE-MPC, and the rule-based baseline. The top row shows temperature evolution relative to the comfort band, and the bottom row reports CO_2 trajectories relative to the IAQ limit.

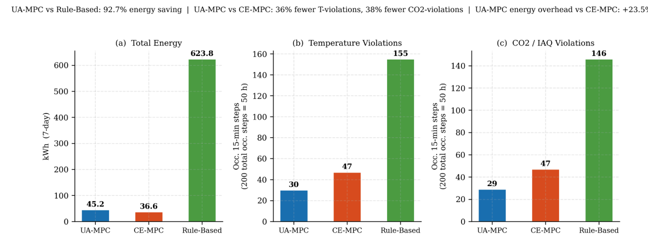

Fig. 5: Aggregate seven-day comparison of energy use, temperature violations, and CO_2/IAQ violations. The proposed UA-MPC reduces comfort and IAQ violations relative to CE-MPC while remaining substantially more efficient than the rule-based baseline.

error with near-nominal interval coverage, indicating that the controller receives uncertainty estimates that are both informative and empirically calibrated. In parallel, the thermal-comfort classifier in Fig. 3 achieves balanced multi-class performance with interpretable feature structure, supporting its role as a supervisory comfort signal rather than a purely descriptive auxiliary model.

C. Closed-Loop Behavior in Representative Operating Windows

Figure 4 reports three representative two-day windows corresponding to Monday–Tuesday, Wednesday–Thursday, and Friday–Saturday operating conditions. Across these scenarios, UA-MPC exhibits tighter tracking of the comfort band than the rule-based baseline and more effective suppression of CO_2 excursions than CE-MPC during challenging occupancy periods. The contrast is especially visible near the onset of occupied intervals, where CE-MPC reacts later because it does not preserve the upper-tail occupancy risk represented in the calibrated intervals. These traces illustrate the mechanism behind the aggregate gains: UA-MPC anticipates occupancy-driven excursions earlier than CE-MPC while using substantially less energy than the rule-based baseline. They show that UA-MPC responds earlier than CE-MPC under occupancy uncertainty while remaining substantially less wasteful than the threshold-driven rule-based baseline.

D. Aggregate Performance and Trade-Off Analysis

The aggregate seven-day comparison in Fig. 5 clarifies the main robustness–energy trade-off of the proposed framework. UA-MPC consumes 45.2 kWh over the evaluation period, compared with 36.6 kWh for CE-MPC and 623.8 kWh for the rule-based controller. Accordingly, UA-MPC is not the minimum-energy solution relative to CE-MPC; it incurs a 23.5% supervisory energy overhead. However, it still achieves a 92.7% energy reduction relative to the rule-based baseline. This additional energy use is accompanied by improved environmental protection. Relative to CE-MPC, UA-MPC reduces temperature violations from 47 to 30 and CO_2 violations from 47 to 29, corresponding to reductions of 36% and 38%, respectively. Since CE-MPC corresponds to median-occupancy operation, this comparison provides a practical sensitivity check for α: the $\alpha = 0.75$ setting improves robustness at a 23.5% energy cost relative to CE-MPC. Relative to the rule-based baseline, UA-MPC also reduces temperature and CO_2 violations from 155 to 30 and from 146 to 29, respectively. Thus, UA-MPC shifts the controller toward a more protective comfort–IAQ policy under calibrated occupancy uncertainty rather than minimizing energy alone. This trade-off should not be interpreted as universally favorable across all building types and climates. The relative benefit of UA-MPC is expected to be strongest in buildings or zones where occupancy uncertainty has a strong effect on both internal heat gains and ventilation demand, such as meeting rooms, classrooms, dense open offices, and intermittently occupied shared spaces. In these settings, underestimating occupancy can quickly produce both temperature discomfort and CO_2 excursions, so a risk-aware controller can justify a moderate energy premium.

In contrast, the benefit may be smaller in buildings with low occupancy variability, low occupant density, weak coupling between occupancy and ventilation demand, or HVAC loads dominated primarily by weather rather than internal gains. Similarly, buildings with highly effective demand-controlled ventilation may already compensate for occupancy changes, reducing the incremental advantage of uncertainty-aware MPC. The present results therefore demonstrate a favorable trade-off for the evaluated operational setting, but broader claims require validation across multiple building typologies, climates, ventilation systems, and occupancy-density regimes.

E. Cross-Scenario Consistency

Figure 6 reports mean ± standard deviation across five two-day windows. This analysis is included to complement the continuous seven-day aggregate evaluation in Fig. 5. The aggregate metric shows the total performance over the evaluation period, whereas the windowed statistics reveal whether the controller remains effective under different short-term occupancy patterns. This distinction is important because

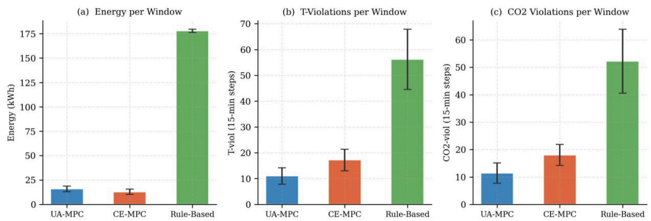

Fig. 6: Mean $\pm$ standard deviation over five two-day windows. The windowed statistics summarize cross-scenario variability and show whether the closed-loop gains persist across different occupancy patterns rather than only in the aggregate seven-day evaluation.

a controller may perform well on average while still being sensitive to particular operating windows.

The five two-day windows were selected to sample multiple representative operating conditions while keeping the analysis compact enough for a six-page conference paper. Two-day windows preserve the temporal structure of occupied and unoccupied periods, including occupancy onset, daily variation, and carry-over effects between consecutive days. Reporting more continuous traces would reduce readability without necessarily clarifying whether the gains are scenario-dependent. The variability in Fig. 6 provides an additional robustness indicator. UA-MPC maintains lower mean temperature and CO_2 violation counts than the rule-based baseline and shows less scenario-dependent fluctuation. This suggests that calibrated occupancy information allows the controller to anticipate occupancy-driven disturbances rather than reacting only after thresholds are exceeded. By contrast, the rule-based controller exhibits higher variability because its threshold-driven logic is more sensitive to the timing and intensity of occupancy changes. Therefore, the five-window analysis indicates that the reported gains are not caused by a single favorable operating period. Instead, UA-MPC provides a more stable comfort and IAQ benefit across different short-term scenarios, although this robustness still comes with the energy premium discussed in Fig. 5.

V. Conclusion

This paper presented an uncertainty-aware adaptive control framework for human-centric cyber-physical indoor spaces by combining conformalized occupancy prediction, PMV-based thermal-comfort classification, and risk-averse interval MPC on an identified thermal/IAQ model. In the seven-day evaluation, UA-MPC reduced temperature violations from 47 to 30 and CO_2 violations from 47 to 29 relative to CE-MPC, with a 23.5% energy overhead, while remaining substantially more efficient than the rule-based baseline. Several limitations remain. The evaluation is based on offline simulation in a single operational setting, so the robustness–energy trade-off may vary with building type, climate, occupancy density, and ventilation design. The RC thermal/IAQ model is reduced-order, the risk parameter α and spatial weights are design choices, and the PMV classifier represents population-level comfort rather than individual preferences. Live deployment may further introduce sensor noise, actuator delays, model drift, computational latency, and privacy constraints. Future work will address online recalibration, adaptive model updating, privacy-preserving occupancy sensing, occupant-preference personalization, and validation across multiple building types and HVAC configurations.

References

[1] A. N. Sayed *et al.*, "Deep and transfer learning for building occupancy detection: A review and comparative analysis," *Engineering Applications of Artificial Intelligence*, 2022. [Online]. Available: https://www.sciencedirect.com/science/article/pii/S0952197622003207

[2] M. Jacoby, S. Y. Tan, G. P. Henze, *et al.*, "A high-fidelity residential building occupancy detection dataset," *Scientific Data*, vol. 8, p. 280, 2021, doi: 10.1038/s41597-021-01055-x.

[3] A. P. Singh and S. Chaudhari, "Room Occupancy Estimation," *UCI Machine Learning Repository dataset*, 2018, doi: 10.24432/C5P605. [Online]. Available: https://archive.ics.uci.edu/dataset/864/room+occupancy+estimation

[4] J. Kim *et al.*, "Occupancy estimation using IoT sensors and machine learning: Incorporating ventilation system operating state and preprocessed differential pressure data," *Building and Environment*, 2023. [Online]. Available: https://www.sciencedirect.com/science/article/abs/pii/S0360132323010065

[5] M. Borrotti *et al.*, "Quantifying Uncertainty with Conformal Prediction for Heating and Cooling Load Forecasting in Building Performance Simulation," *Energies*, vol. 17, no. 17, p. 4348, 2024, doi: 10.3390/en17174348.

[6] P. Michailidis *et al.*, "Model Predictive Control for Smart Buildings: Applications and Innovations," *Buildings*, vol. 15, no. 18, p. 3298, 2025, doi: 10.3390/buildings15183298.

[7] A. Soleimanijavid, I. Konstantzos, and X. Liu, "Challenges and opportunities of occupant-centric building controls in real-world implementation: A critical review," *Energy and Buildings*, vol. 308, p. 113958, 2024, doi: 10.1016/j.enbuild.2024.113958.

[8] S. Yang *et al.*, "An adaptive robust model predictive control for indoor climate optimization and uncertainties handling in buildings," *Building and Environment*, 2019. [Online]. Available: https://www.sciencedirect.com/science/article/abs/pii/S0360132319305360

[9] G. Hu and F. You, "Multi-zone building control with thermal comfort constraints under disjunctive uncertainty using data-driven robust model predictive control," *Advances in Applied Energy*, p. 100124, 2023, doi: 10.1016/j.adapen.2023.100124.

[10] N. He *et al.*, "Stochastic model predictive control for the optimal operation of office buildings," *Building and Environment*, 2025. [Online]. Available: https://www.sciencedirect.com/science/article/abs/pii/S0360132324010904

[11] J. Liu *et al.*, "Model Predictive Control for Coupled Indoor Air Quality and Energy Performance Based on Incremental Thermal Preference Learning: Experimental Validation in Office Environments," *Sustainability*, vol. 18, no. 1, p. 240, 2026, doi: 10.3390/su18010240.

[12] V. F. Ličina *et al.*, "Development of the ASHRAE Global Thermal Comfort Database II," *Building and Environment*, 2018. [Online]. Available: https://www.sciencedirect.com/science/article/abs/pii/S0360132318303652

[13] Z. Q. Fard *et al.*, "Application of machine learning in thermal comfort studies: A review of methods, performance and challenges," *Energy and Buildings*, 2022. [Online]. Available: https://www.sciencedirect.com/science/article/abs/pii/S0378778821010550

[14] W. Zhang *et al.*, "A review on occupancy prediction through machine learning for enhancing energy efficiency, air quality and thermal comfort in the built environment," *Renewable and Sustainable Energy Reviews*, 2022.

[15] Z. Wang *et al.*, "An occupant-centric control strategy for indoor thermal comfort, air quality and energy management," *Energy and Buildings*, 2023, doi: 10.1016/j.enbuild.2023.112899.

[16] Z. Wang *et al.*, "Multi-objectives occupant-centric control of thermostats and natural ventilation systems in cold climate conditions using real-time occupant-related information," *Building and Environment*, 2024.

[17] H. Zhang *et al.*, "Stochastic occupancy-integrated MPC for multi-objective optimal built environment control," *Building Simulation*, 2025.